Published in final edited form as:
Otolaryngol Head Neck Surg. 2012 June ; 146(6): 938–945. doi:10.1177/0194599812436648.

Microbubble Therapy Enhances Anti-tumor Properties of Cisplatin and Cetuximab In Vitro and In Vivo

Cara H. Heath, MD[1], **Anna Sorace, MS**[2], **Joseph Knowles, MD**[1], **Eben Rosenthal, MD**[1], and **Kenneth Hoyt, PhD, MBA**[2,3]

[1]Department of Surgery, University of Alabama at Birmingham, Birmingham, Alabama, USA

[2]Biomedical Engineering, University of Alabama at Birmingham, Birmingham, Alabama, USA

[3]Radiology, University of Alabama at Birmingham, Birmingham, Alabama, USA

Abstract

Objective—To determine if microbubble-mediated ultrasound therapy (MB-UST) can improve cisplatin or cetuximab cytotoxicity of head and neck squamous cell carcinoma (HNSCC) in vitro and in vivo by increasing tumor-specific drug delivery by disruption of tumor cell membranes and enhancing vascular permeability.

Study Design—In vitro and in vivo study.

Setting—University medical center.

Subjects—Immunodeficient mice (6 weeks old) and 4 HNSCC cell lines.

Methods—Changes to cell permeability were assessed in vitro after MB-UST. Cellular apoptosis resulting from adjuvant MB-UST with subtherapeutic doses of cisplatin or cetuximab was assessed by cell survival assays in vitro. The in vivo effect of adjuvant MB-UST in flank tumors was assessed in vivo with histological analysis and diffusion-weighted magnetic resonance imaging (DW-MRI).

Results—In vitro results revealed that MB-UST can increase cell permeability and enhance drug uptake and apoptosis in 4 HNSCC cell lines. In vivo adjuvant MB-UST with cetuximab or cisplatin showed a statistically significant reduction in tumor size when compared with untreated controls. TUNEL analysis yielded a larger number of cells undergoing apoptosis in tumors treated with cetuximab and adjuvant MB-UST than did cetuximab alone but was not significantly greater in tumors treated with cisplatin and adjuvant MBUST compared with cisplatin alone. DW-MRI analysis showed more free water, which corresponds to increased cell membrane disruption, in tumors treated with MB-UST.

Corresponding Author: Kenneth Hoyt, PhD, Divisions of Radiology and Biomedical Engineering, 1808 7th Av South, Birmingham, AL 35294-0012, USA, hoyt@uab.edu.

This work was presented at the 2011 AAO-HNSF Annual Meeting & OTO EXPO; September 11–14, 2011; San Francisco, California.

Author Contributions

Cara H. Heath, study design, acquisition of data, data analysis, drafting and approval; **Anna Sorace**, study design, acquisition of data, data analysis, drafting and approval; **Joseph Knowles**, study design, acquisition of data, data analysis, drafting and approval; **Eben Rosenthal**, study design, drafting, and approval; **Kenneth Hoyt**, study design, drafting, and approval.

Disclosures

Competing interests: None.

Sponsorships: None.

Conclusion—MB-UST promotes disruption of cell membranes in tumor cells in vitro, which may be leveraged to selectively improve the uptake of conventional and targeted therapeutics in vivo.

Keywords

ultrasound; microbubbles; head and neck squamous cell carcinoma; cetuximab; cisplatin

Head and neck squamous cell carcinoma (HNSCC) is the fifth most common cancer worldwide, with an estimated global incidence of 533,100 new cases including more than 40,000 people in the United States diagnosed annually.[1–3] During the past 20 years, treatments for HNSCC have gradually evolved to combining surgery, radiotherapy, and chemotherapy. Cisplatin is one of the most frequently used chemotherapeutic agents in the treatment of HNSCC, and the antitumor activity is dependent on its ability to cross the cell membrane. A combined multimodality approach, including the addition of conventional chemotherapy (eg, cisplatin) to radiation, has improved disease outcomes but with significant patient morbidity and an increase in treatment-related deaths.[4,5]

More recent advancements in therapies for HNSCC have emerged since the identification of new molecular targets that are specific for head and neck carcinomas. One of these new targets includes the epidermal growth factor receptor (EGFR). EGFR is a tyrosine kinase receptor that has been found highly expressed in HNSCC and has been associated with more advanced disease and less favorable outcomes.[6,7] These discoveries led to the development of novel therapeutics such as cetuximab, which is a monoclonal antibody that enters the tumor and targets the extracellular domain of EGFR. Study results have shown modest outcome improvements in HNSCC treated with cetuximab, especially when used in combination with radiotherapy.[8]

Despite advancements in the treatment of HNSCC with novel targeted therapeutics and combined treatment regimens, toxicities still contribute significantly to patient morbidity. The toxic drugs pose limitations on treatment by exerting their effects on normal tissue, resulting in toxicities and dose-limiting side effects.[9,10] There is a need for combined treatment regimens with nonoverlapping toxicities or treatment regimens that increase drug delivery and uptake in diseased tissues while sparing normal tissue.

Recently, a technique known as microbubble-mediated ultrasound therapy (MB-UST) has been explored in other cancer types as a potential modality to locally enhance drug delivery at the tumor site.[11–13] Microbubbles (MBs) are ultrasound contrast agents that function as intravascular tracers. They are made of a protein, starch, lipid, or polymer shell filled with inert gas. Definity MBs are commercially available and approved by the US Food and Drug Administration for cardiac outflow applications. It is known that exposure of MBs to a properly timed ultrasound field results in mechanical oscillations that can disrupt nearby endothelial cell membranes and temporarily enhance vascular permeability. It is hypothesized that MB-UST increases permeability of cells by the membrane disruption induced by MB-UST, thereby allowing intracellular uptake of exogenous membrane-impermeable molecules. The treatment of HNSCC with adjuvant MB-UST may subsequently enhance the antitumor effectiveness of chemotherapeutic and biologically targeted treatment by increasing cell permeability and tumor uptake of chemotherapeutic agents, resulting in enhanced drug delivery to diseased tissue while minimizing the harmful systemic side effects of the toxic drugs.

Methods

Cell Lines, Culture, and Transformation Methods

This work was approved by the University of Alabama at Birmingham Institutional Animal Care and Use Committee (IACUC). The head and neck cancer cell lines SCC-1, SCC-5, Cal27, and FaDu were grown and maintained under appropriate culture conditions using proper aseptic techniques.[14] Cell lines were maintained in DMEM, 10% FBS, 1% L-glutamine, and 1% Pen/Strep (Sigma, St Louis, MO). Cells were grown at 37°C, with 5% CO_2 and 90% relative humidity. All cells were cultured to 70% to 90% confluence before passage. Appropriate cell numbers for in vitro assays were determined using flow cytometry (Accuri C6; Accuri Cytometers Inc, Ann Arbor, MI). The FaDu cell line was established from a squamous cell carcinoma of the pharynx (ATCC, Manassas, VA). The SCC-1 cell line was established from a squamous cell carcinoma from the floor of the mouth, and the SCC-5 cell line was established from a primary tumor of the supraglottis. The SCC-1 and SCC-5 cell lines were provided by Thomas Carey, PhD, University of Michigan, Ann Arbor.

The SCC-1 cell line was chosen for transfection with a lentivirus containing both puromycin resistance and luciferase genes.[15] Briefly, SCC-1 cells were plated in a 24-well plate 24 hours prior to viral infection at a density of 0.5×10^5 cells per well in 0.5 mL of complete DMEM medium (with serum and antibiotics). Lentivirus was thawed in a 37°C water bath and prepared in a mixture of complete medium with Polybren (concentration of 5 μg/mL). Media were aspirated from plate wells and replaced with 0.5 mL of this prewarmed Polybrene/media mixture per well (for the 24-well plate). Cells were infected by adding 10 μL of viral stock. The infected target cells were selected for stable expression using puromycin. Luciferase expression was assessed by Xenogen 200 series IVIS photon counter (Caliper Life Sciences, Hopkington, MA) after adding 150 μg/mL D-luciferin (Gold Biotechnology, St Louis, MO) in the culture medium. Puromycin selection pressure was used to generate stable SCC-1 cell lines.

In Vitro Ultrasound Therapy and Luciferin Uptake

MB-UST was administered in vitro under conditions previously described by Sorace et al.[13] Briefly, 50 μL of activated microbubbles (concentration of 14 million MBs/mL; Definity, Lantheus Medical Imaging, Billerica, MA) was added to cells grown in acoustically transparent flasks (Opticell, Rochester, NY). Immediately after administration of MBs, flasks were inverted and immersed in a water bath at 37°C opposite a 0.75-inch immersion transducer (Olympus, Waltham, MA) in series with a signal generator (AFG3022B; Tektronix, Beaverton, OR) and power amplifier (A075; Electronics and Innovation, Rochester, NY). Cells were exposed to an ultrasound field for 5 minutes at a transient frequency of 1.0 MHz, a mechanical index of 0.5, a pulse repetition period of 0.01 seconds, and a duty cycle of 20%.

To look at luciferin uptake, SCC-1 cells expressing the luciferase gene were grown on acoustically transparent flasks. After 24 hours, 30 μg luciferin was added. MB-UST was administered to half of the flasks. Control flasks were administered MBs and subjected to the same conditions, but ultrasound was not used. Luciferase expression was assessed again using the Xenogen photo counter.

In Vitro Cellular Uptake and Viability

Cisplatin (NovaPLUS, Irving, TX) was conjugated to an Alexa680 fluorphore (Invitrogen, Carlsbad, CA) by separation column chromatography, while cetuximab (Imclone, New York, NY) was conjugated to Cy5.5. MBs were administered to plated cells (1×10^6) using combination MB-UST and 10 μM cisplatin or 10 μM cetuximab therapy. Control cells

underwent no therapy, monotherapy with cisplatin, cetuximab, or UST alone. Following a 24-hour incubation period, cells were washed using phosphate-buffered saline and assessed for fluorescence using an Olympus 1X70 microscope (Olympus American, Melville, NY).

After treatment, SCC-1, SCC-5, FaDu, and Cal27 cells were trypsinized and stained for viability and death using calcein AM and propidium iodide (BD Biosciences, Franklin Lakes, NJ). Cells were then stained with 1.0 μL of working calcein-AM stock (50 μL) and incubated for 15 minutes in 37°C. After incubation, 2.0 μL of 0.5 mg/mL propidium iodide was added. Cells were analyzed for viability by fluorescence counts (10k event) using flow cytometry. All experimental groups were analyzed in triplicate.

In Vivo Ultrasound Therapy

Athymic female nude mice (6 weeks old) were obtained (Jackson Laboratories, Bar Harbor, ME). SCC-5 cells (2×10^6) were implanted in the left flank of 30 mice. Three weeks postimplant, mice were sorted into the following 6 groups (n = 5): no treatment (control), UST alone, 10 μM cisplatin, 100 μM cetuximab, 10 μM cisplatin + UST, and 100 μM cetuximab + UST. All reagents were delivered by intravenous tail vein injection. UST consisted of administering 100 μL of MBs (Definity) followed by US exposure in a 37°C water bath using the setup described in the in vitro methods but with a pulse repetition period of 5 seconds (Figure 1).[13] The control group received 100 μL saline injections. Mice remained under isoflurane anesthesia for the entirety of the experiment. Therapy occurred twice weekly for 4 weeks and was followed by weight and digital caliper measurements of tumor size. On days 0, 14, and 28, tumors were assessed by diffusion-weighted magnetic resonance imaging (DW-MRI; Bruker 9.4T MR, Bruker Corp, Billerica, MA). On day 28, animals were euthanized and tumors excised for histological analysis.

Immunohistologic Analysis

Serial sections of 5-μm thickness from tumor samples were cut from formalin-fixed, paraffin-embedded tissue blocks and floated onto charged glass slides (Super-Frost Plus; Fisher Scientific, Waltham, MA). Antigen retrieval was performed with 0.01 M Tris-1 mM EDTA buffer (pH 9) using a pressure cooker. Endogenous peroxidase was blocked with 3% hydrogen peroxide for 10 minutes. After blocking, all slides were then incubated at 4°C overnight with either Ki67, TUNEL, or CD31 antibody. Negative controls were achieved by eliminating the primary antibodies from the diluents. Following washing with TBST, peroxidase-conjugated goat antirabbit IgG (for CD31, TUNEL, and Ki67; 1:200, Jackson ImmunoResearch, West Grove, PA) was applied to the sections for 30 minutes at room temperature. Diaminobenzidine (Scy Tek Laboratories, Logan, UT) was used as the chromagen and hematoxylin (7211; Richard-Allen Scientific, Kalamazoo, MI) as the counterstain.

Statistical Analysis

Data were summarized as mean ± SE. Statistical analyses were performed using JMP 7.1 (SAS, Cary, NC) software. Analysis of in vitro cell death, fluorescent uptake, and histological staining was performed using a χ^2 analysis of variance, while luciferase expression, tumor size, and DW-MRI were analyzed using a 2-sample t test. A P value less than .05 was considered statistically significant.

Results

MB-Mediated Ultrasound Therapy Disrupts Cell Membranes In Vitro

Transmembrane migration of a small molecule, luciferin (the substrate for luciferase), was used to determine the amount of disruption of cell membranes. Enhanced luciferin uptake

following MB-UST was demonstrated with a luciferase-positive SCC-1 head and neck cancer cell line. Comparison of luciferase expression between the control and therapy groups showed a 41% increase in luciferin uptake in cells receiving MB-UST as compared with control ($P < .001$; Figure 2A). In vitro results also demonstrated that adjuvant MB-UST can increase intracellular drug concentrations of fluorescently labeled cisplatin and cetuximab. Cetuximab with adjuvant MB-UST demonstrated a 28% intracellular increase compared with treatment with cetuximab in the absence of MB-UST ($P = .01$). Cisplatin with adjuvant MB-UST revealed a 9% increase over control counterparts without MB-UST ($P = .67$; Figure 2B).

After determining that MB-UST can disrupt cell membranes and the cytotoxic effects of cisplatin and cetuximab with adjuvant MB-UST by examining cellular apoptosis in 4 HNSCC cell lines in vitro (SCC-1, SCC-5, FaDu, and Cal27), a dose curve for one cell line was established. Results showed that adjuvant MB-UST enhances the cytotoxic effect of cisplatin and cetuximab in all 4 head and neck cancer cell lines (Figure 3A). Fluorescent images of propidium iodine–stained SCC-5 cells showed qualitative analysis of viable and dead cells. The representative images showed increased fluorescent red expression (dead cells), signifying an increased amount of apoptosis when using adjuvant MB-UST (Figure 3B). Enhanced drug uptake in SCC-5 cells resulted in a significant leftward shift in the dose-response curves. This shift was greatest at the 1-μM dose for cisplatin and 10-μM dose of cetuximab (Figure 3C).

In Vivo Drug Uptake

In vivo treatment of xenografted tumors using MB-UST demonstrated an inhibition of tumor growth in comparison to animals receiving chemotherapeutic drug (cisplatin or cetuximab) alone, MB-UST alone, or no treatment ($P < .05$). Mice that underwent MB-UST alone revealed no significant difference in tumor size following treatment when compared with untreated controls ($P = .81$). Also, groups treated with either cetuximab or cisplatin alone showed a reduction in tumor size, but the difference was not statistically significantly different compared with controls ($P = .15$ and $P = .06$, respectively). However, tumors treated with adjuvant MB-UST in addition to cetuximab or cisplatin were significantly smaller than control ($P = .02$ and $P = .01$, respectively). Although the addition of MB therapy to cetuximab or cisplatin did reduce tumor size, this effect was not significant ($P = .19$, $P = .20$). Tumors treated with cetuximab and adjuvant MB-UST exhibited a 26% decrease in tumor size at termination compared with cetuximab alone ($P = .05$). Tumors treated with cisplatin and adjuvant MBUST presented a 21% decrease in tumor size when compared with cisplatin alone ($P = .24$; Figure 4). There was no tissue damage observed in any of the surrounding tissues in any of the mice treated with MB-UST.

Histologic Analysis Using TUNEL, CD-31, and Hematoxylin and Eosin Staining

TUNEL analysis yielded a larger number of cells undergoing apoptosis in tumors treated with cetuximab and adjuvant MB-UST than cetuximab alone (55% vs 44%, $P = .015$) but was not significantly greater in tumors treated with cisplatin and adjuvant MB-UST compared with cisplatin alone (84% vs 77%, $P = .24$; Figure 5C). Although hematoxylin and eosin staining did not show changes in vascular morphology, there was a positive correlation between microvessel density and reduction in tumor size ($P = .05$). Comparisons between drug and drug + MB-UST group data revealed no statistically significant differences in tumor vascularity (CD31) measurements ($P > .05$). This indicates that existing tumor vascularity did not affect UST results (Figure 5A,B).

DW-MRI

Intratumoral apoptosis and early-phase cell wall disruption was assessed per tumor volume from the adjusted diffusion coefficient (ADC) values obtained from DW-MRI on days 0, 14, and 28. ADC values are known to correspond to disruption of cell membranes and release of free water into the tumor mass and can be used as an early predictor of response to therapy in HNSCC.[5,16] Significant increases in ADC values were found in tumors treated with cetuximab and adjuvant MB-UST from cetuximab alone ($P = .001$) and cisplatin and adjuvant MB-UST and cisplatin alone ($P = .001$) (Figure 6). These changes in the ADC values suggest an increase in cell wall rupture associated with MB-UST therapy.

Discussion

Currently the overall effectiveness of chemotherapeutic agents is determined by their ability to penetrate tissues and cross cell membranes. This effectiveness is compromised by insufficient delivery of drug to the tumor microenvironment and by the side effects of delivering the drug to normal tissues. Our current studies show that adjuvant MB-UST can increase the efficacy of HNSCC chemotherapeutics, such as cetuximab and cisplatin. This technique may be leveraged to adjust dosing of conventional and targeted therapeutics to allow treatment with subtherapeutic drug concentrations and therefore decrease toxicity. As MB-UST is a localized treatment like radiation and surgery, it can be used on any disease that is localized. The effects of MB-UST allow a site-specific method to increase drug uptake, and the localized nature of treatment also means localized toxicity.

MB-UST may increase the therapeutic efficacy of these agents by causing a transient increase in tumor permeability and therefore increase the uptake of exogenous molecules into the tumor.[13,17] This application has also been shown to be effective in the delivery of small molecules and genetic material into cells.[13,18,19] The proposed mechanism of action is through mechanical vibration of MBs using US, whereby membrane disruption and tumor permeability are temporarily induced.[20] This effect has been demonstrated previously by increased cellular uptake of small fluorescent molecules and labeled chemotherapeutic agents.[19] In the current in vitro experiments, we were able to use a membrane-impermeable fluorescent molecule to demonstrate the effects that MB-UST has on extracellular small-molecule uptake. Results show that MB-UST was sufficient to increase molecule uptake by showing a 41% increase in luciferase expression secondary to an increase in membrane permeability.

In vitro results also show that MB-UST increases the uptake of 2 fluorescently labeled drugs, cisplatin and cetuximab, resulting in an increase in drug delivery and apoptosis. The in vivo results suggest that adjuvant MB-UST has an additive effect with cetuximab and cisplatin, as demonstrated by a statistically significant reduction of tumor size in these treatment groups. The enhancement of cisplatin uptake with adjuvant MB-UST is possibly attributed to the transient porous membrane created by MB-UST, thereby facilitating more drug entry into the nucleus. The increased cytotoxicity seen with cetuximab and adjuvant MB-UST may be secondary to increased uptake in the tumor from the MB-UST–induced increase in vascular permeability or by changes in cell signaling. To assess the response to MB-UST, we investigated the use of DW-MRI as an imaging technique to assess tumors. In vivo data from DW-MRI analysis showed a statistically significant increase in ADC values associated with MB-UST treatment. These ADC values correlate with an increase in free water in the tumor secondary to a loss of cell wall integrity.

Combining different treatment modalities has been shown to improve locoregional control of HNSCC; however, at the same time, this can increase overall toxicity. In particular, it has been shown that the addition of cetuximab to either radiotherapy or cisplatin will potentiate

the toxic effects of either therapy. We can overcome this limitation by delivering the drug only to the tumor itself by using site-specific MB-UST to enhance drug delivery into HNSCC cells. It has been shown in previous studies that MB-UST can be effective at delivering drugs and transferring genetic material into cells for potential treatment in breast, prostate, and colon cancer,[13,21–23] and we are now able to demonstrate this effect in HNSCC. The effect cannot be described as synergistic as MB-UST is not applicable to the synergy effects as described by Chou.[24] We are outside of this statistical analysis since MB-UST alone without drug has no effect. However, MB-UST can produce an additive effect with nonoverlapping toxicity. In vitro studies show that we can use lower doses of a therapeutic agent and see a cytotoxicity profile similar to higher doses.

In conclusion, we show that MB-UST can be effective in increasing drug uptake and thereby apoptosis in HNSCC in vitro and in vivo. This application can allow the use subtherapeutic doses of cetuximab and cisplatin without reducing the clinical efficacy of the drugs. We also conclude from our imaging results that DW-MRI may be a potential tool for monitoring the response to combination MB-UST and drug therapy.

Acknowledgments

Funding source: This work was supported by the National Institutes of Health (2T32 CA091078-06).

References

1. Ang KK, Trotti A, Brown BW, et al. Randomized trial addressing risk features and time factors of surgery plus radiotherapy in advanced head-and-neck cancer. Int J Radiat Oncol Biol Phys. 2001; 51:571–578. [PubMed: 11597795]
2. Seiwert TY, Cohen EE. State-of-the-art management of locally advanced head and neck cancer. Br J Cancer. 2005; 92:1341–1348. [PubMed: 15846296]
3. American Cancer Society. Cancer Facts and Figures. Atlanta, GA: American Cancer Society; 2010 Oct 3. 2010.
4. Cohen EE, Lingen MW, Vokes EE. The expanding role of systemic therapy in head and neck cancer. J Clin Oncol. 2004; 22:1743–1752. [PubMed: 15117998]
5. Forastiere AA, Goepfert H, Maor M, et al. Concurrent chemotherapy and radiotherapy for organ preservation in advanced laryngeal cancer. N Engl J Med. 2003; 349:2091–2098. [PubMed: 14645636]
6. Salomon DS, Brandt R, Ciardiello F, et al. Epidermal growth factor-related peptides and their receptors in human malignancies. Crit Rev Oncol Hematol. 1995; 19:183–232. [PubMed: 7612182]
7. Herbst RS, Langer CJ. Epidermal growth factor receptors as a target for cancer treatment: the emerging role of IMC-C225 in the treatment of lung and head and neck cancers. Semin Oncol. 2002; 29:27–36. [PubMed: 11894011]
8. Bonner JA, Harari PM, Giralt J, et al. Radiotherapy plus cetuximab for squamous-cell carcinoma of the head and neck. N Engl J Med. 2006; 354:567–578. [PubMed: 16467544]
9. Logan RM. Advances in understanding of toxicities of treatment for head and neck cancer. Oral Oncol. 2009; 45:844–848. [PubMed: 19467918]
10. Elting LS, Keefe DM, Sonis ST, et al. Patient-reported measurements of oral mucositis in head and neck cancer patients treated with radiotherapy with or without chemotherapy: demonstration of increased frequency, severity, resistance to palliation, and impact on quality of life. Cancer. 2008; 113:2704–2713. [PubMed: 18973181]
11. Escoffre JM, Piron J, Novell A, et al. Doxorubicin delivery into tumor cells with ultrasound and microbubbles. Mol Pharm. 2011; 8:799–806. [PubMed: 21495672]
12. Haag P, Frauscher F, Gradl J, et al. Microbubble-enhanced ultrasound to deliver an antisense oligodeoxynucleotide targeting the human androgen receptor into prostate tumours. J Steroid Biochem Mol Biol. 2006; 102:103–113. [PubMed: 17055720]

13. Sorace AG, Warram J, Umphrey H, Hoyt K. Ultrasonic techniques for improved chemotherapeutic delivery in cancer. J Drug Target. 2012; 20:43–54. [PubMed: 21981609]
14. Lin CJ, Grandis JR, Carey TE, et al. Head and neck squamous cell carcinoma cell lines: established models and rationale for selection. Head Neck. 2007; 29:163–188. [PubMed: 17312569]
15. Karuppiah M. Transient transfection and luciferase assay. Protocol Exchange. 2006 http://www.nature.com/protocolexchange/protocols/115.
16. Koh DM, Collins DJ. Diffusion-weighted MRI in the body: applications and challenges in oncology. Am J Roentgenol. 2007; 188:1622–1635. [PubMed: 17515386]
17. Karshafian R, Bevan PD, Williams R, et al. Sonoporation by ultrasound-activated microbubble contrast agents: effect of acoustic exposure parameters on cell membrane permeability and cell viability. Ultrasound Med Biol. 2009; 35:847–860. [PubMed: 19110370]
18. Frenkel V. Ultrasound mediated delivery of drugs and genes to solid tumors. Adv Drug Deliv Rev. 2008; 60:1193–1208. [PubMed: 18474406]
19. Deckers R, Yudina A, Cardoit LC, et al. A fluorescent chromophore TOTO-3 as a “smart probe” for the assessment of ultrasound-mediated local drug delivery in vivo. Contrast Media Mol Imaging. 2011; 6(4):267–274. [PubMed: 21861287]
20. Schlicher RK, Hutcheson JD, Radhakrishna H, et al. Changes in cell morphology due to plasma membrane wounding by acoustic cavitation. Ultrasound Med Biol. 2010; 36:677–692. [PubMed: 20350691]
21. Aoi A, Watanabe Y, Mori S, et al. Herpes simplex virus thymidine kinase-mediated suicide gene therapy using nano/microbubbles and ultrasound. Ultrasound Med Biol. 2008; 34:425–434. [PubMed: 18096302]
22. Gao Z, Kennedy AM, Christensen DA, et al. Drug-loaded nano/microbubbles for combining ultrasonography and targeted chemotherapy. Ultrasonics. 2008; 48:260–270. [PubMed: 18096196]
23. Watanabe Y, Aoi A, Horie S, et al. Low-intensity ultrasound and microbubbles enhance the antitumor effect of cisplatin. Cancer Sci. 2008; 99:2525–2531. [PubMed: 19018767]
24. Chou TC. Drug combination studies and their synergy quantification using the Chou-Talalay method. Cancer Res. 2010; 70:440–446. [PubMed: 20068163]

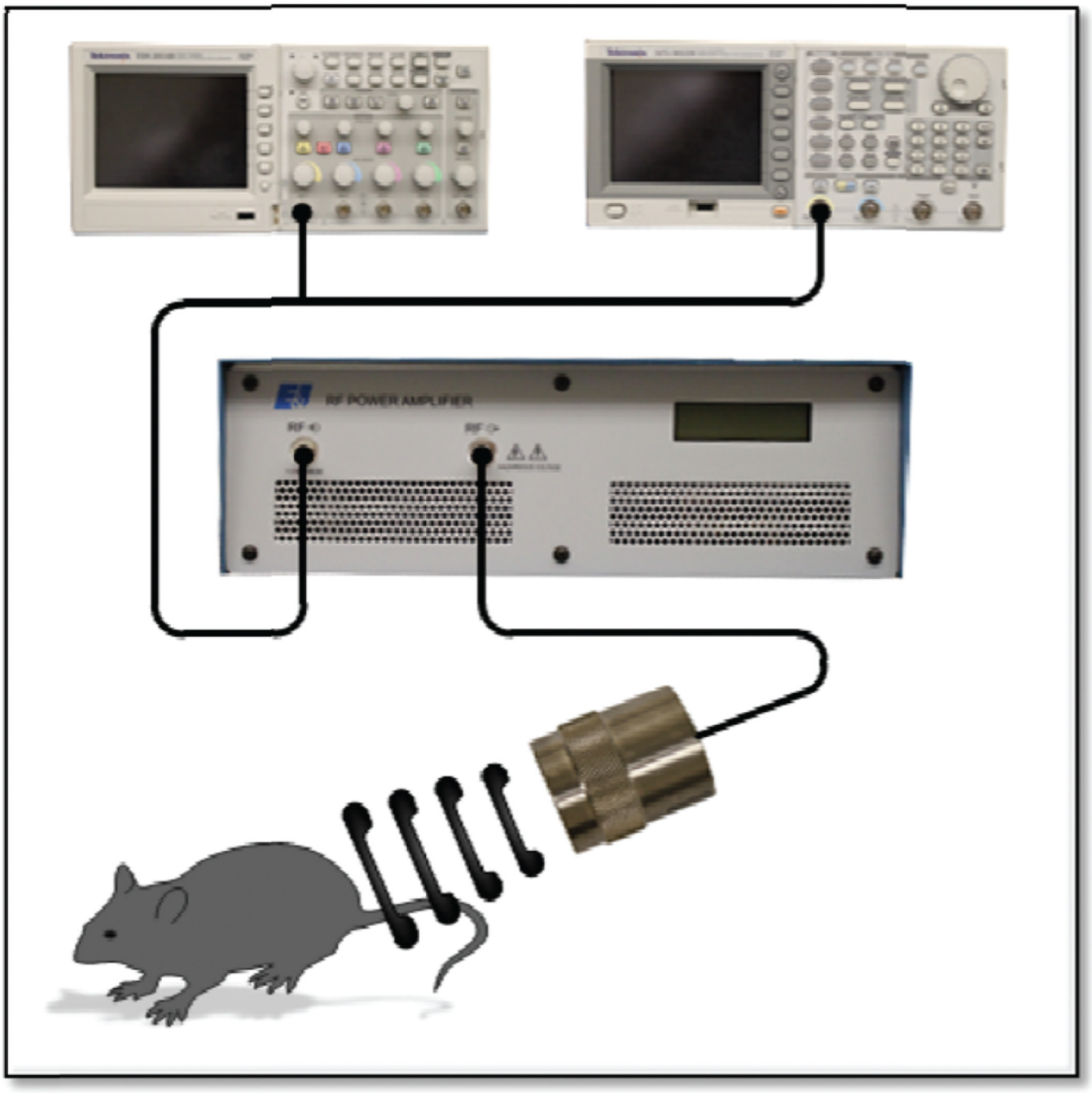

Figure 1.
Experimental setup for microbubble-mediated ultrasound therapy.

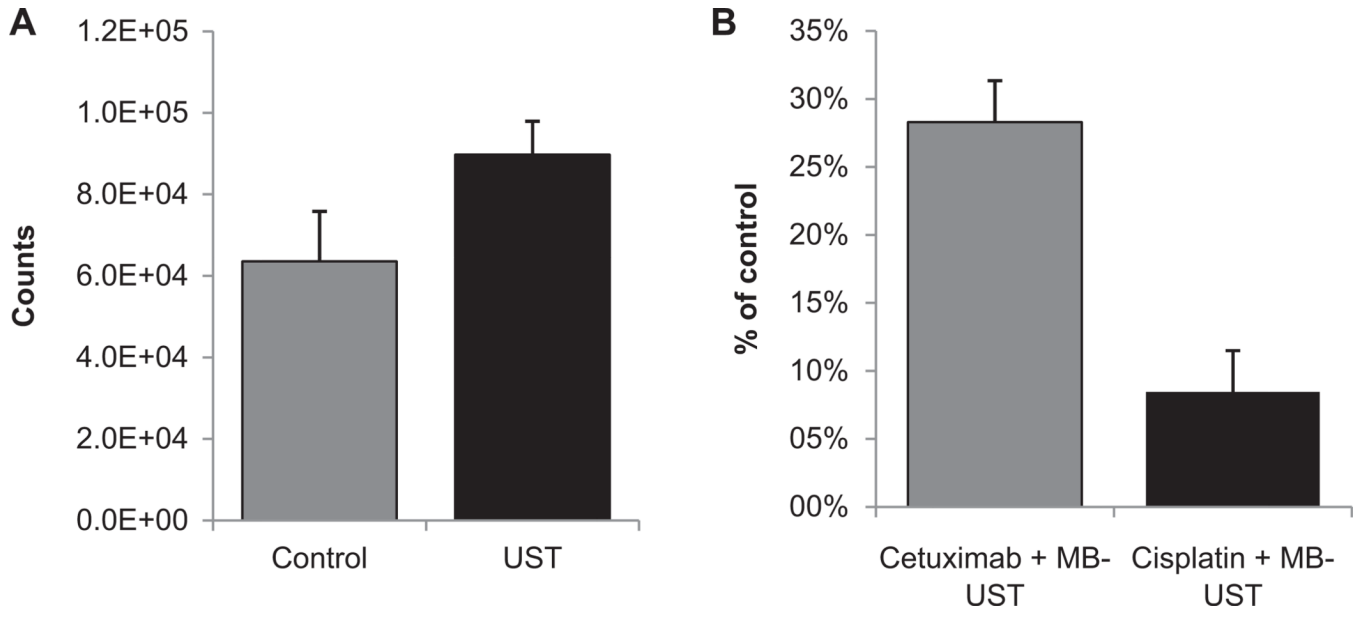

Figure 2.

(A) Bioluminescence of luciferase-positive SCC-1 cells after microbubble-mediated ultrasound therapy (MB-UST). SCC-1 cells showed increased fluorescence following MB-UST when compared with controls with no MB-UST ($P < .001$). (B) Fluorescently labeled drug uptake with cetuximab and cisplatin following MB-UST. SCC-1 cells treated with MB-UST and fluorescently labeled cetuximab showed a statistically significant increase in drug uptake as compared with controls receiving MB-UST alone ($P = .02$). There was also an increase in cisplatin uptake, although it was not statistically significant ($P = .3$). Error bars represent standard error.

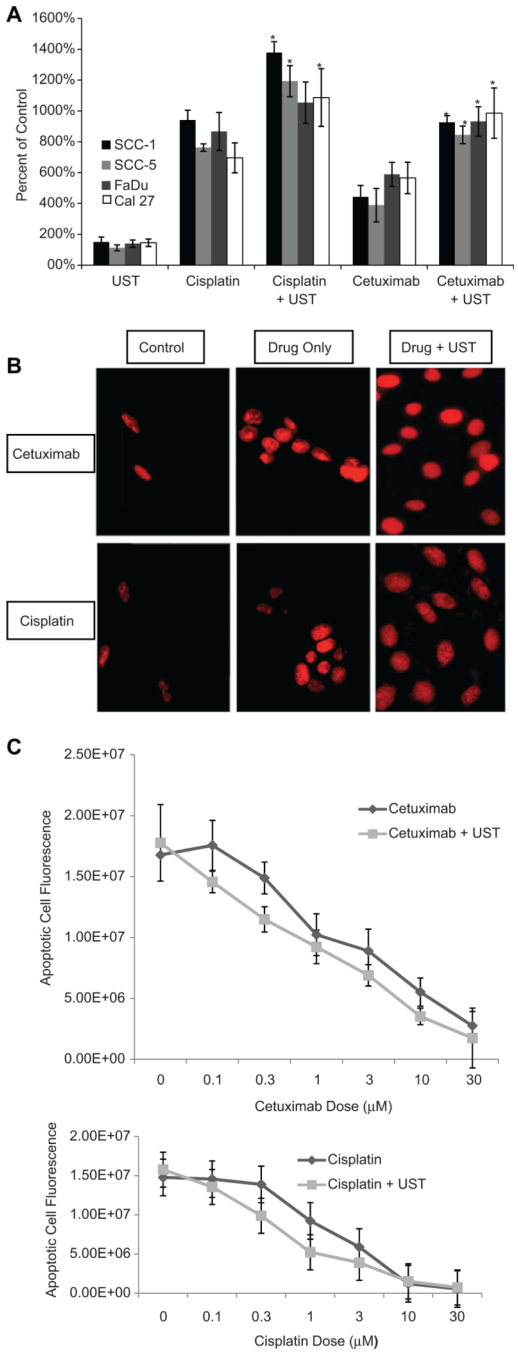

Figure 3.

(A) Quantitative analysis of apoptosis as percentage of untreated control in head and neck squamous cell carcinoma cell lines (SCC-1, SCC-5, FaDu, and Cal27). Cells were treated with ultrasound only (UST), cisplatin (1 μM) only, cisplatin plus UST, cetuximab (10 μM) only, or cetuximab plus UST. In all 4 cell lines treated with combination drug and microbubble-mediated ultrasound therapy (MB-UST), there was statistically more apoptosis (*$P < .05$). (B) Quantitative analysis of apoptosis using propidium iodide (PI) in SCC-5 cells. Cotreatment with MB-UST significantly increased cell death with both cetuximab ($P < .05$) and cisplatin ($P < .05$). (C) Dose-response curves for SCC-5 cells in the presence of cetuximab and UST and cisplatin and UST.

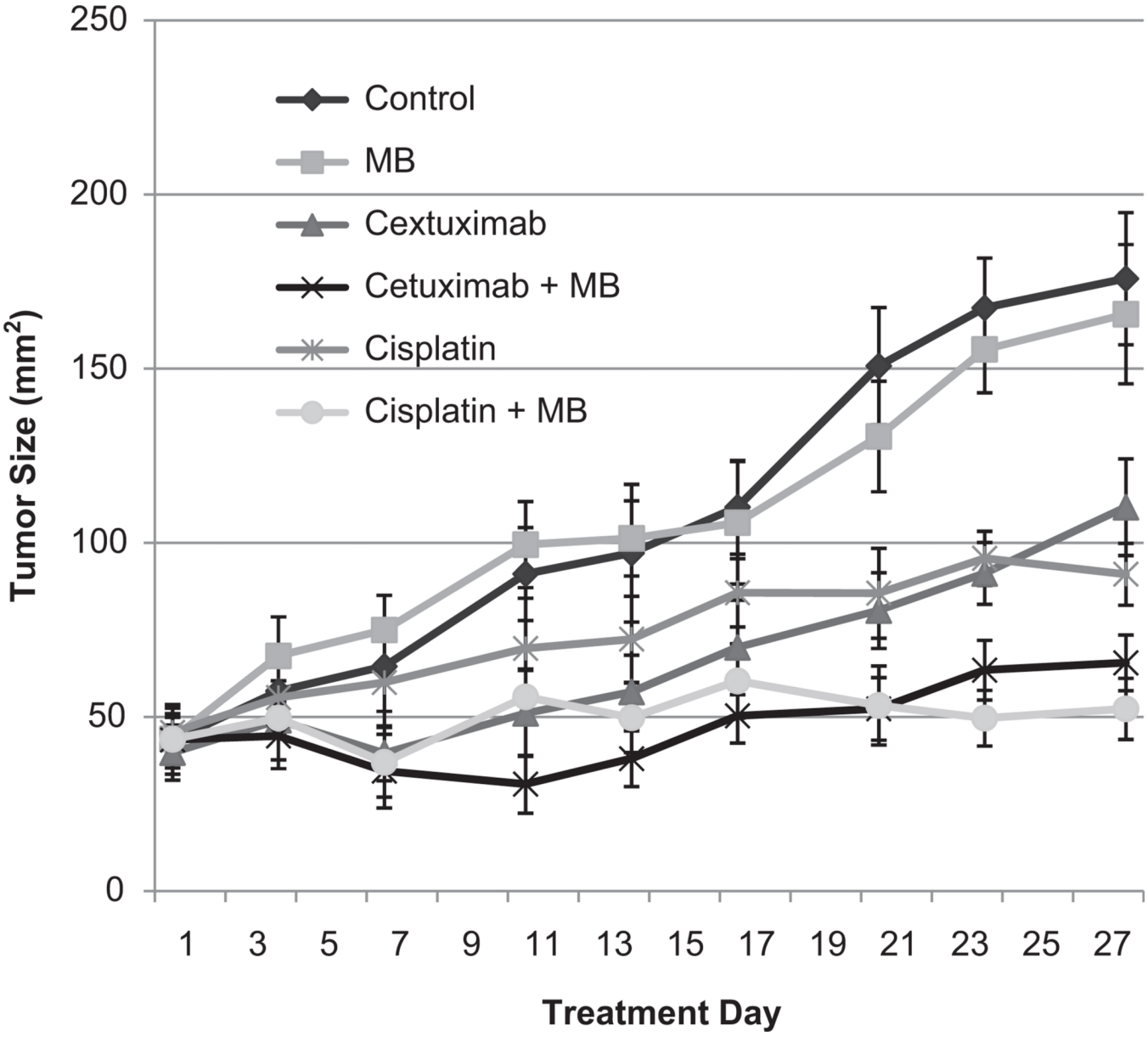

Figure 4.

In vivo microbubble-mediated ultrasound therapy (MB-UST) and cetuximab and cisplatin treatment on SCC-5 tumors. Tumors treated with cetuximab and adjuvant MB-UST exhibited a decrease in tumor size at termination compared with cetuximab alone ($P = .05$). Tumors treated with cisplatin and adjuvant MB-UST decreased in tumor size when compared with cisplatin alone ($P = .24$). Error bars represent standard error.

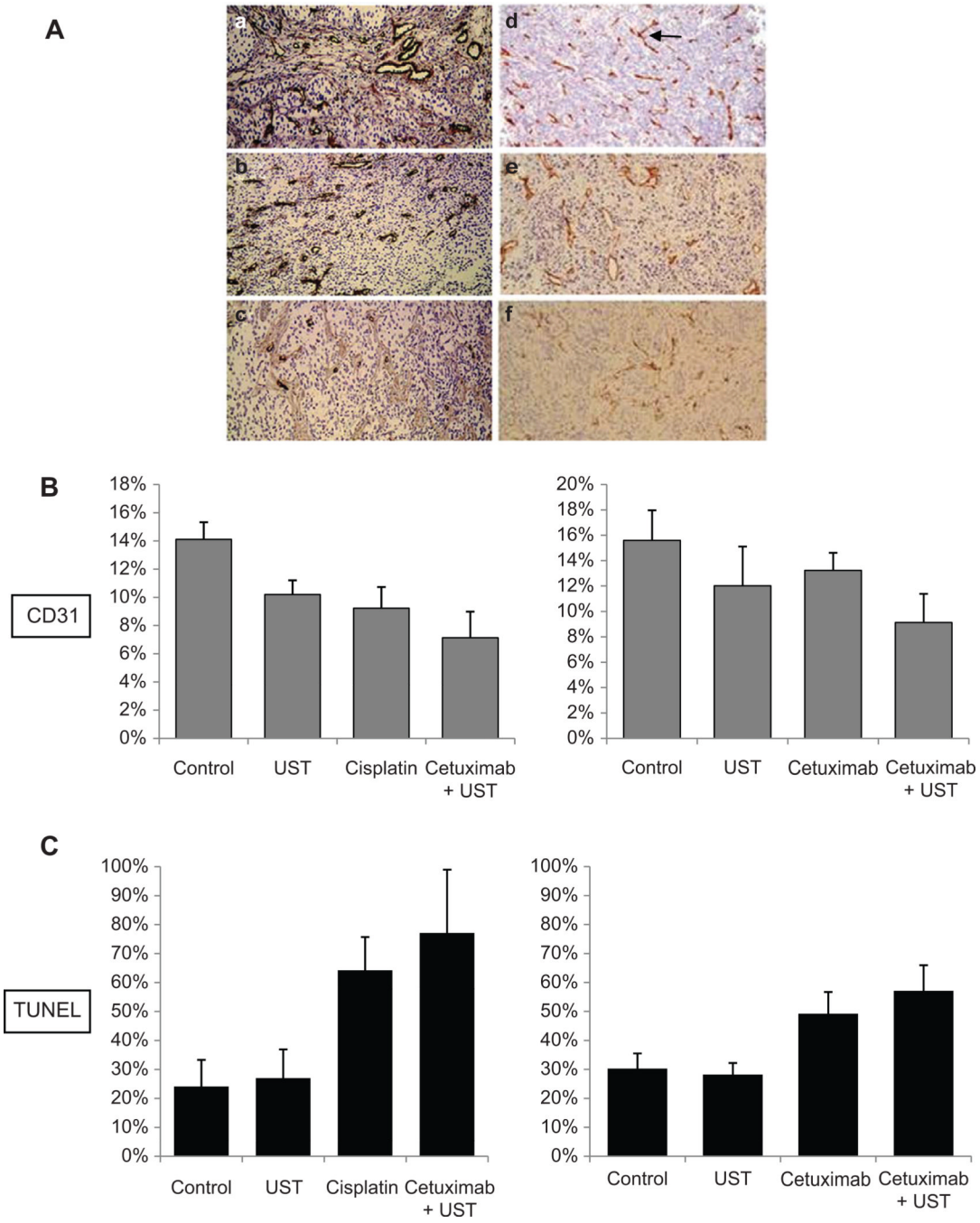

Figure 5.

(A) CD31 microvessel staining in SCC-5 flank tumors with no treatment (a), cetuximab (b), cetuximab + MB-mediated UST (c), microbubble-mediated ultrasound therapy (MB-UST) alone (d), cisplatin (e), and cisplatin + MB-mediated UST (f). (B) CD31 staining of SCC5 tumors. (C) TUNEL staining of SCC5 tumors. Error bars represent standard error.

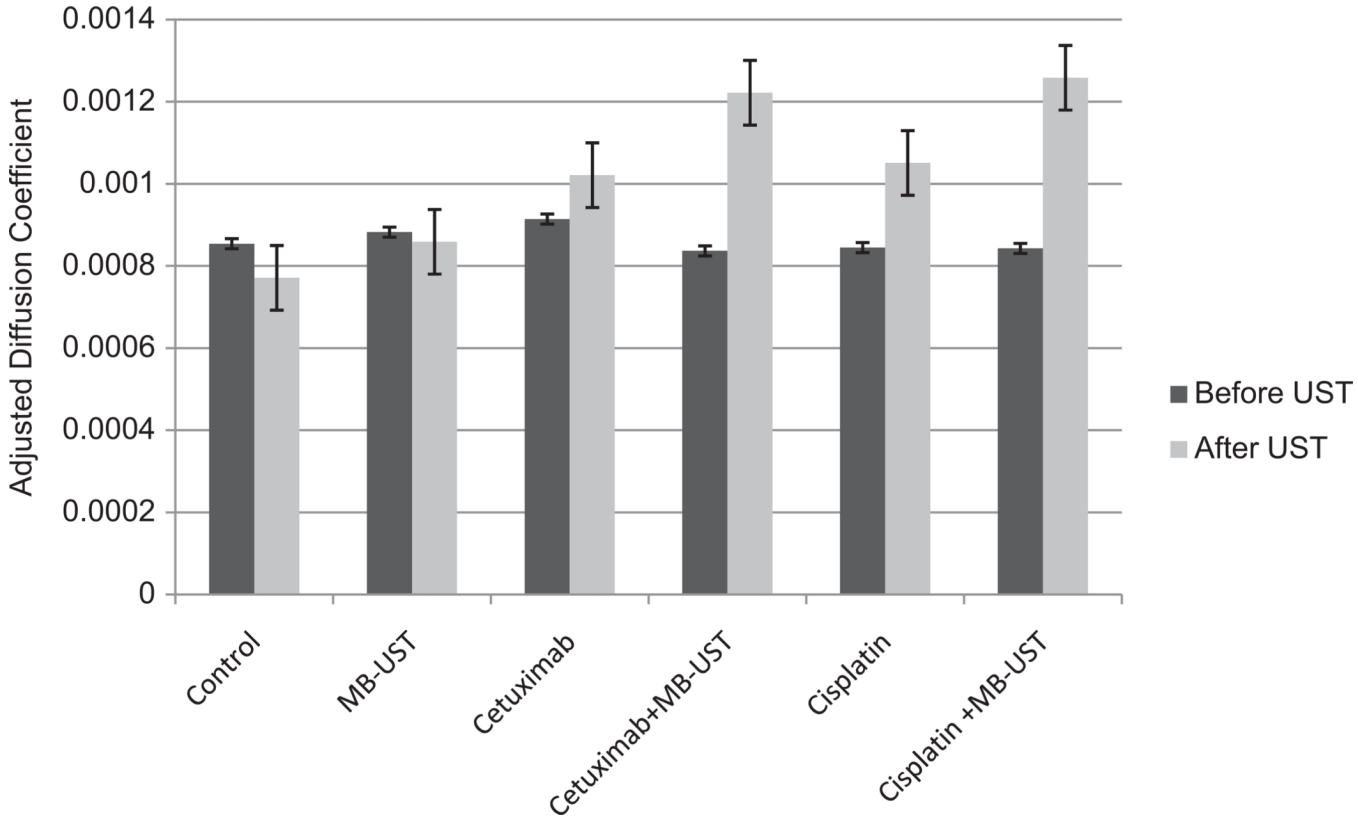

Figure 6.

Diffusion-weighted magnetic resonance imaging adjusted diffusion coefficient values of SCC-5 flank tumors before and after ultrasound treatment. Tumors treated with cisplatin + microbubble-mediated ultrasound therapy (MB-UST) and cetuximab + MB-UST had an increase in free water content, reflected as an increase in the adjusted diffusion coefficient ($P < .001$ and $P = .002$, respectively). Error bars represent standard error.